2013

Investigation of CO, C2H6 and Aerosols in a Boreal Fire Plume Over Eastern Canada During BORTAS 2011 Using Ground- and Satellite-Based Observations and Model Simulations

D. Griffin

K. A. Walker

J. E. Franklin

M. Parrington

C. Whaley

See next page for additional authors

Original Publication Citation

Griffin, D., Walker, K. A., Franklin, J. E., Parrington, M., Whaley, C., Hopper, J., . . . Weaver, D. (2013). Investigation of CO, C_2H_6 and aerosols in a boreal fire plume over eastern Canada during BORTAS 2011 using ground- and satellite-based observations and model simulations. *Atmospheric Chemistry and Physics, 13*(20), 10227-10241. doi: 10.5194/acp-13-10227-2013

Atmos. Chem. Phys., 13, 10227–10241, 2013
www.atmos-chem-phys.net/13/10227/2013/
doi:10.5194/acp-13-10227-2013

Atmospheric Chemistry and Physics Open Access

Investigation of CO, C_2H_6 and aerosols in a boreal fire plume over eastern Canada during BORTAS 2011 using ground- and satellite-based observations and model simulations

D. Griffin[1], K. A. Walker[1,2], J. E. Franklin[3], M. Parrington[4,*], C. Whaley[1], J. Hopper[3], J. R. Drummond[3], P. I. Palmer[4], K. Strong[1], T. J. Duck[3], I. Abboud[5], P. F. Bernath[6,7], C. Clerbaux[8,9], P.-F. Coheur[9], K. R. Curry[3], L. Dan[1], E. Hyer[10], J. Kliever[1], G. Lesins[3], M. Maurice[1], A. Saha[11], K. Tereszchuk[7], and D. Weaver[1]

[1]Department of Physics, University of Toronto, Toronto, Ontario M5S 1A7, Canada
[2]Department of Chemistry, University of Waterloo, Waterloo, Ontario N2L 3G1, Canada
[3]Department of Physics and Atmospheric Science, Dalhousie University, Halifax, Nova Scotia B3H 1Z9, Canada
[4]School of GeoSciences, The University of Edinburgh, Edinburgh EH9 3JN, UK
[5]AEROCAN, Environment Canada, Egbert, Ontario L0L 1N0, Canada
[6]Department of Chemistry and Biochemistry, Old Dominion University, Norfolk, Virginia 23529, USA
[7]Department of Chemistry, University of York, Heslington, York YO10 5DD, UK
[8]UPMC Univ. Paris 06, Université Versailles St.-Quentin, CNRS/INSU, LATMOS-IPSL, Paris, France
[9]Spectroscopie de l'atmosphère, Chimie Quantique et Photophysique, Université Libre de Bruxelles, Brussels, Belgium
[10]Marine Meteorology Division, Naval Research Laboratory, Monterey, California 93943, USA
[11]CARTEL, Université de Sherbrooke, 2500, boulevard de l'Université, Sherbrooke, Québec J1K 2R1, Canada
[*]now at: European Centre for Medium-Range Weather Forecasts, Shinfield Park, Reading, RG2 9AX, UK

Correspondence to: K. A. Walker (kwalker@atmosp.physics.utoronto.ca)

Received: 28 March 2013 – Published in Atmos. Chem. Phys. Discuss.: 24 April 2013
Revised: 19 August 2013 – Accepted: 27 August 2013 – Published: 18 October 2013

Abstract. We present the results of total column measurements of CO, C_2H_6 and fine-mode aerosol optical depth (AOD) during the "Quantifying the impact of **BOR**eal forest fires on **T**ropospheric oxidants over the Atlantic using **A**ircraft and **S**atellites" (BORTAS-B) campaign over eastern Canada. Ground-based observations, using Fourier transform spectrometers (FTSs) and sun photometers, were carried out in July and August 2011. These measurements were taken in Halifax, Nova Scotia, which is an ideal location to monitor the outflow of boreal fires from North America, and also in Toronto, Ontario. Measurements of fine-mode AOD enhancements were highly correlated with enhancements in coincident trace gas (CO and C_2H_6) observations between 19 and 21 July 2011, which is typical for a smoke plume event. In this paper, we focus on the identification of the origin and the transport of this smoke plume. We use back trajectories calculated by the Canadian Meteorological Centre as well as FLEXPART forward trajectories to demonstrate that the enhanced CO, C_2H_6 and fine-mode AOD seen near Halifax and Toronto originated from forest fires in northwestern Ontario that occurred between 17 and 19 July 2011. In addition, total column measurements of CO from the satellite-borne Infrared Atmospheric Sounding Interferometer (IASI) have been used to trace the smoke plume and to confirm the origin of the CO enhancement. Furthermore, the enhancement ratio – that is, in this case equivalent to the emission ratio ($ER_{C_2H_6/CO}$) – was estimated from these ground-based observations. These C_2H_6 emission results from boreal fires in northwestern Ontario agree well with C_2H_6 emission measurements from other boreal regions, and are relatively high compared to fires from other geographical regions. The ground-based CO and C_2H_6 observations were compared with outputs from the 3-D global chemical transport model GEOS-Chem, using the Fire Locating And Modeling of Burning Emissions (FLAMBE) inventory. Agreement within the stated measurement uncertainty ($\sim 3\%$ for

CO and ∼ 8 % for C_2H_6) was found for the magnitude of the enhancement of the CO and C_2H_6 total columns between the measured and modelled results. However, there is a small shift in time (of approximately 6 h) of arrival of the plume over Halifax between the results.

1 Introduction

Large amounts of trace gases as well as aerosols are released from biomass burning. These emissions affect air quality and tropospheric and stratospheric chemistry, which has an important impact on the radiative transfer in the atmosphere (Crutzen and Andreae, 1990). The emissions from biomass burning can be transported thousands of miles downwind, and thus boreal fires in North America can affect the air quality in Europe (Derwent et al., 2004). It has been found that the North American emissions, both natural and anthropogenic (Li et al., 2002), have a significant impact on the air quality in Europe. While the impact of anthropogenic emissions have been studied previously (Li et al., 2002; Stohl and Trickl, 1999), the impact from North American boreal fires is not as well known.

There are several species of interest which are present in boreal fire plumes and are indicators of smoke plumes (Tereszchuk et al., 2011); however, we will focus in our study on carbon monoxide (CO) and ethane (C_2H_6) as well as fine-mode aerosols. All of these species have a relatively long lifetime in the troposphere and can, therefore, be detected up to several thousand kilometres away from the fire source. CO and C_2H_6 generally have a lifetime between 1 and 3 months, which is primarily limited by oxidation by the hydroxyl radical (OH) (Volz et al., 1981; Rudolph and Ehhalt, 1981). Fine-mode (sub-micron) aerosols have a shorter lifetime that is dependent upon their size, latitudinal location and altitude in the atmosphere. In the troposphere, fine-mode aerosols of a medium size (approximately 0.15 µm) are removed from the troposphere by wet deposition, and thus their lifetime is limited by precipitation. The average lifetime is approximately 3–5 days at mid-latitudes (Edwards et al., 2006). Smaller aerosols, with sizes of the order of 0.01 µm, coagulate first to larger particles, and are then removed by wet deposition. The different trace gases, as well as aerosols, are emitted simultaneously during a biomass burning event; therefore, the enhancements in the total columns of the emitted gases will correlate quite well until the various lifetimes of the gases or aerosols cause the correlation to break down (Paton-Walsh et al., 2008). Therefore, trace gases (CO and C_2H_6) and the fine-mode aerosol optical depth (AOD) should be highly correlated within fire plumes that are less than 3–5 days old (where this is limited by the lifetime of the aerosols).

A number of previous studies have focused on the emission factors (EFs) and emission ratios (ERs) of several trace gases during biomass burning events. Emission ratios are used in model simulations, and have a significant influence on the output of atmospheric models. The work of Andreae and Merlet (2001) identifies emission factors and ratios for almost 100 species for different geographical regions, which are commonly used for model simulations. Akagi et al. (2011) published an update to this paper, which has a finer categorization of fire regions, and combines laboratory experiments with field measurements from aircraft and ground-based instruments. Significant differences in the emission ratio and therefore in the emission factor of C_2H_6 have been found for biomass burning for different geographical regions. As an example, the emissions of C_2H_6 from Australian and African bush fires are comparatively low (Paton-Walsh et al., 2005; Sinha et al., 2003), whereas C_2H_6 emissions from boreal and temperate fires seem to be comparatively high (Akagi et al., 2011). The variability and the uncertainty of these emission ratios is quite high, even within a precisely defined area. Differences can occur for the same fire events, which are likely due to different emissions into different altitudes; as such, aircraft and satellite measurements can differ from ground-based in situ observations (Akagi et al., 2011).

In this work, we use ground-based Fourier transform spectrometer (FTS) and sun photometer measurements to investigate in a case study of a boreal fire plume in July 2011. These measurements have been taken as part of the "Quantifying the impact of **BOR**eal forest fires on **T**ropospheric oxidants over the Atlantic using **A**ircraft and **S**atellites" (BORTAS) project. BORTAS was a 4 yr project, including a 2 yr measurement phase which was carried out during July and August of 2010 and 2011 (phases A and B, respectively). It is currently the most recent campaign that focussed on the impact of North American boreal fires on tropospheric composition and their influence on European air quality. Further details on the campaign can be found in Palmer et al. (2013). Ground-based measurements during this campaign were primarily taken at the Dalhousie Ground Station (DGS). This facility was located on the roof of the Sir James Dunn building at Dalhousie University (44.64° N, 63.59° W, 65 m a.s.l.) in Halifax, Nova Scotia, Canada. As part of the DGS, two FTSs and a CIMEL sun photometer were operated simultaneously. Having these co-located instruments facilitates the comparison and evaluation of the correlation between CO, C_2H_6 and AOD. During the BORTAS-B campaign in 2011, enhancements of CO, C_2H_6 and the fine-mode AOD could be detected on three days: 19, 20 and 21 July 2011. On the same days, enhancements in C_2H_6 were detected over Toronto by the FTS located at the University of Toronto Atmospheric Observatory (TAO: 43.66° N, 79.40° W, 174 m a.s.l.) in Toronto, Ontario, Canada.

This paper investigates the boreal fire plume which passed over Halifax and Toronto between 19 and 21 July 2011. We use back trajectories calculated by the Canadian Meteorological Centre (CMC) and FLEXPART forward trajectories, as well as CO total column measurements from the satellite-borne Infrared Atmospheric Sounding Interferometer (IASI),

to show that these enhancements originated from boreal fires in northwestern Ontario between 17 and 19 July 2011. In this study, the emission ratio and emission factor of C_2H_6 are calculated from ground-based FTS measurements and compared to two recent studies (within the BORTAS project) of the emission ratio and emission factor from airborne and satellite observations (Lewis et al., 2013; Tereszchuk et al., 2013). Furthermore, this paper compares results from the chemical transport model GEOS-Chem to the ground-based FTS observations.

This paper is organized as follows. Subsequent to this introduction, the second section introduces the different instruments and measurement sites used in the campaign, data analysis and the retrieval methods. In the third section, the measurement time series are presented, and the retrievals are compared with the other instruments. The fourth section discusses the results of this study. Here, the transport and origin of the smoke plume are identified using model simulations (CMC, FLEXPART). Furthermore, the correlation between the trace gases and the fine-mode AOD as well as the emission factors from our ground-based observations and the comparison between these observations and GEOS-Chem simulations are discussed. This is followed by a summary of our results in the last section.

2 Methodology and datasets

For the analysis of the smoke plume observed during the BORTAS-B campaign in July 2011, we use measurements taken in Halifax and Toronto. This section focuses on the instruments, retrieval processes and the methods used for the instrument comparisons, as well as on the chemical transport model GEOS-Chem, to which the observations are compared.

The observations were taken at DGS using two FTSs (the Portable Atmospheric Research Interferometric Spectrometer for the Infrared (PARIS-IR) and the Dalhousie Atmospheric Observatory DA8; herein the DAO-DA8) and a CIMEL sun photometer. Additionally, observations from a second DA8 (TAO-DA8) and a second CIMEL sun photometer were used, both of which are located in Toronto. However, these two instruments are not co-located. The TAO-DA8 is operated at the University of Toronto, while the sun photometer is located at Environment Canada (43.97° N, 79.47° W, 300 m a.s.l.). These ground-based FTSs are dedicated to infrared solar absorption measurements from direct sunlight. For these observations, a solar beam is directed into each instrument using a suntracking mirror system located on the roof of the building. Details of each of the instruments and the data analysis technique are given below.

2.1 The Portable Atmospheric Research Interferometric Spectrometer for the Infrared (PARIS-IR)

PARIS-IR is a ground-based FTS which is based on the design of the Atmospheric Chemistry Experiment Fourier Transform Spectrometer (ACE-FTS) (Fu et al., 2007). It measures atmospheric solar absorption spectra between 750 and 4400 cm^{-1}, and operates at a maximum spectral resolution of 0.02 cm^{-1} (at a maximum optical path difference (MOPD) of $\pm$25 cm). Interferograms are recorded using liquid-nitrogen-cooled mercury cadmium telluride (HgCdTe) and indium antimonide (InSb) detectors configured in a sandwich arrangement. The beam splitter is made from zinc selenide (ZnSe). No filters are used, which means that the entire spectral range (750–4400 cm^{-1}) is measured simultaneously for each observation. No apodization is applied to the spectra. Each measurement, which is comprised of 20 co-added spectra, is taken approximately every 7 min (Sung et al., 2007). Therefore, CO is measured every 7 min throughout the campaign whenever weather conditions are favourable. Due to the high water vapour absorption over Halifax and the spectral resolution of 0.02 cm^{-1}, it is not possible to retrieve C_2H_6 total columns reliably from the PARIS-IR spectra taken at DGS.

2.2 ABB Bomem DA8 FTSs

The DAO-DA8 FTS at DGS is a vertically aligned Michelson interferometer (Franklin et al., 2013). It is equipped with InSb and HgCdTe detectors and a potassium bromide (KBr) beam splitter to provide spectral coverage between 750 and 4500 cm^{-1}. Its maximum spectral resolution is 0.004 cm^{-1} (at a MOPD of 250 cm). Six narrow-band filters (typically 700–1000 cm^{-1} in width) are used to improve the signal-to-noise ratio (SNR) of the spectra. Depending on the filter used, typically four to six spectra are co-added. Measurements using one filter are taken over approximately 6 min. Due to the different narrow band filters, CO (filter 4: 2000–2700 cm^{-1}) and C_2H_6 (filter 3: 2400–3100 cm^{-1}) are measured approximately every hour, depending on the weather conditions.

A second, very similar DA8 is operated at the University of Toronto (TAO-DA8) (Wiacek et al., 2007). For this instrument, measurements using one filter require approximately 20 min. Therefore, CO (filter 4) and C_2H_6 (filter 3) are typically measured every 2–3 h, as weather conditions allow.

2.3 Data analysis for the FTS spectra

For these three FTSs, a similar retrieval technique has been applied to estimate the total column amounts from the recorded solar absorption spectra. This retrieval method is based on an optimal estimation method (OEM) (Rodgers, 1976, 2000), where a calculated spectrum is fitted to the observed one by adjusting the target trace gas profile. Multiple

microwindows, typically each with a width between 0.3 and 1.0 cm^{-1}, are employed simultaneously in the retrieval process. This analysis has been applied to the observed spectra from the three FTSs described above using the SFIT2 v3.94c retrieval package (Pougatchev et al., 1995, 1996) and the HITRAN 2008 spectroscopic database (Rothman et al., 2009). Total column amounts were calculated from the retrieved volume mixing ratio (VMR) profiles by integrating the atmospheric density and the trace gas VMR throughout the altitude range (from the ground to 100 km). Due to the lower resolution of PARIS-IR compared to the DA8 FTSs, two different altitude grids have been used for the retrieval. The retrievals performed with spectra from PARIS-IR use a 29-layer grid, and those for the DA8s use a 48-layer grid. It has been shown that this prevents non-physical oscillations in the retrieved profile for the lower resolution FTS, but only results in a very small difference in the total columns (between 0.1 and 0.6 % depending on the retrieved gas) (Wunch et al., 2007). Daily pressure and temperature profiles, specific to each measurement site, are taken from the National Centers for Environmental Prediction (NCEP) re-analyses available through the NASA Goddard Space Flight Center automailer (http://hyperion.gsfc.nasa.gov/Data_services/automailer/index.html) and then are linearly interpolated on the desired altitude grid. The a priori profiles of trace gases, which are used for all retrievals, are the mean of a 40 yr run (1980–2020) of the Whole Atmosphere Community Climate Model (WACCM; Eyring et al., 2007) for Halifax and Toronto (J. Hannigan, NCAR, personal communication, 2012), v6 and v5, respectively. The SNR, for the determination of the measurement covariance matrix, is instrument specific, and values are selected for each gas by applying a trade-off curve method described by Batchelor et al. (2009).

The microwindows used and interfering trace gases taken into account for the retrieval are listed in Table 1. These are consistent for all of the FTS retrievals, and are based on the Network for Detection of Atmospheric Composition Change (NDACC) standard microwindows. Furthermore, Table 1 lists the estimated uncertainties as well as the degrees of freedom of signal (DOFS) of each retrieval. The DOFS are defined as the trace of the averaging kernel matrix. The uncertainties are derived using a method similar to that described by Batchelor et al. (2009) and Sung et al. (2007). The smoothing error, the measurement error and the uncertainties of the line width and line intensity parameters of the retrieved trace gas from HITRAN 2008 (Rothman et al., 2009) are included in this calculation. Furthermore, the error caused by the uncertainty of the interfering trace gases and that caused by the retrieval parameters, specifically the error due to the temperature uncertainty (2 K) and the uncertainty of the solar zenith angle SZA (0.125°), are considered. The total uncertainty has been estimated by adding all errors in quadrature.

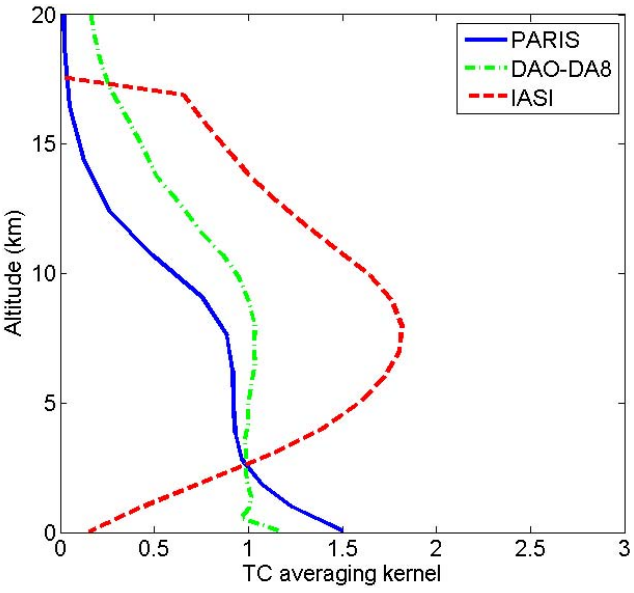

Fig. 1. Typical total column (TC) averaging kernels for CO for PARIS-IR (solid blue line), DA8 (dot-dashed green line) and IASI during a morning overpass (dashed red line).

2.4 IASI

Launched in October 2006, the IASI instrument onboard the polar-orbiting MetOp-A satellite is a nadir-viewing high-resolution FTS (Clerbaux et al., 2009). It records infrared emission spectra between 645 and 2760 cm^{-1} with an apodized spectral resolution of 0.5 cm^{-1}. IASI provides global coverage twice daily.

The IASI CO vertical profiles and total columns are retrieved with FORLI-CO, which has been developed at the Université Libre de Bruxelles (ULB). Similar to the retrievals for the ground-based FTSs, FORLI-CO uses an OEM based on Rodgers (2000). The spectral range between 2143 and 2181.25 cm^{-1} is used for the CO retrieval, and it is performed on a 19-layer altitude grid (Hurtmans et al., 2012). The CO profiles provide between 1.5 and 2 independent pieces of information (DOFS), for mid-latitudes, for which the uncertainty of the CO retrieval varies between 3 and 9 % (George et al., 2009; Turquety et al., 2009). The IASI CO output has previously been used to detect the CO emission caused by fires (e.g. Krol et al., 2013).

For this study, total column CO from IASI has been used. For the comparisons shown here, all satellite measurements within a longitudinal and latitudinal area of $\pm 0.5°$ (approximately ± 55 km) around the ground-based measurement site have been used.

Table 1. Summary of retrieval microwindows and interfering species, with an estimate of the uncertainty of the retrieval and DOFS for each FTS. In each retrieval, multiple microwindows are fitted simultaneously as listed in the table below. For the calculation of the total uncertainty and contributions, see the description given in the text.

Gas	Microwindows (cm^{-1})	Interfering Species	Total uncertainty (%)			DOFS		
			PARIS	DAO-DA8	TAO-DA8	PARIS	DAO-DA8	TAO-DA8
CO	2057.70–2058.00 2069.56–2069.90 2157.50–2158.60	O_3, CO_2, OCS, N_2O, H_2O	2.9	2.6	2.6	1.4	1.5	1.5
C_2H_6	2976.66–2976.95 2983.20–2983.55 2986.50–2986.95	H_2O, O_3	N/A	7.7	7.7	N/A	1.0	1.5

2.5 Intercomparison between FTSs

The effect of the different resolutions of the FTSs is accounted for in this study. Generally, for lower resolution spectrometers, the retrievals have lower vertical resolution (fewer DOFS), which means the profile typically corresponds to a total column. The total column averaging kernels of typical PARIS-IR, DAO-DA8 and IASI CO retrievals are shown in Fig. 1. PARIS-IR is sensitive to CO in the lowest layers of the atmosphere between approximately 0 and 10 km, whereas the DAO-DA8 is sensitive between approximately 0 and 15 km. The averaging kernels demonstrate that the ground-based instruments have the highest sensitivity to CO in the layers close to the surface, where IASI has the highest sensitivity towards CO between approximately 5 and 15 km.

The effect of the different averaging kernels on the total columns can be accounted for using a similar method to Rodgers and Connor (2003). The profile $\boldsymbol{x}_{\mathrm{h}}$, retrieved by the spectrometer, having higher vertical sensitivity (DAO-DA8 and IASI), is linearly interpolated onto the PARIS-IR retrieval grid and smoothed with its averaging kernel, $\mathbf{A}$, and a priori profile, $\boldsymbol{x}_{\mathrm{a}}$, using

$$\boldsymbol{x}_{\mathrm{smooth}} = \boldsymbol{x}_{\mathrm{a}} + \mathbf{A} \cdot (\boldsymbol{x}_{\mathrm{h}} - \boldsymbol{x}_{\mathrm{a}}). \quad (1)$$

The total column for these smoothed profiles has been calculated from the smoothed VMR profile $\boldsymbol{x}_{smooth}$ and the atmospheric density using the same method as for the unsmoothed profiles (see Sect. 2.3).

2.6 AEROCAN/AERONET

The ground-based AOD measurements were obtained by AEROCAN, a Canadian subnetwork of the AErosol RObotic NETwork (AERONET) (Holben et al., 1998). Data across the network are acquired by a CIMEL Electronique 318A sun photometer. Direct sunlight measurements are taken across eight narrow spectral bands in the ultraviolet, visible and near-infrared spectral region. The typical time interval between measurements is 3 min for AEROCAN measurements under favourable weather conditions.

The fine- (sub-micron) and coarse- (super-micron) mode AOD are obtained from these measurements using a spectral deconvolution algorithm developed by O'Neill et al. (2003), which is applied to a five-wavelength subset of the CIMEL bands (380, 440, 500, 675 and 870 nm). The enhancement of fine-mode AOD is a signature indicator of smoke events, which makes it possible to study the enhancement of aerosols associated with the boreal fire plumes, while excluding AOD enhancements due to super-micron aerosols and clouds (identified by an enhancement of coarse-mode AOD). The errors of the fine-mode AOD were computed using the error model defined in O'Neill et al. (2003), and are based on an average pan-spectral AOD error of 0.01. The estimated total errors for the fine-mode AOD are typically between 15 and 30 %. Level 1.0 (non-cloud-screened) data were employed for this analysis (data which were corrected for post-season recalibration). While the issue of cloud screening is less problematic for fine-mode data, use of these retrievals avoids the accidental "cloud screening" of highly variable smoke AODs that can be induced by the standard, temporally based AERONET cloud-screening algorithm.

2.7 GEOS-Chem global 3-D chemistry transport model

GEOS-Chem is a global 3-D chemical transport model that utilizes assimilated meteorological fields from the NASA Goddard Earth Observing System (GEOS) (Bey et al., 2001). As was used by Parrington et al. (2012), we use v8-02-04 of GEOS-Chem with a horizontal resolution of 2° latitude × 2.5° longitude, 48 vertical levels and hourly output. The GEOS-5 meteorological fields employed here have a horizontal resolution of 0.5° latitude × 0.67° longitude, 72 vertical levels (from the surface up to 0.01 hPa) and a temporal resolution of 6 h (3 h for surface variables). The biomass burning emissions are taken from the Fire Locating And Modeling of Burning Emissions (FLAMBE) inventory (Reid et al., 2009). The carbon emissions from FLAMBE have been aggregated to a 1° × 1° horizontal grid globally, which

are then re-gridded to the resolution of GEOS-Chem. For the model simulation, individual aerosol and trace gases from biomass burning emissions are scaled with the emission factors from Andreae and Merlet (2001).

In this study, we examine the model results in three nearby grid boxes. This is done because Halifax is located in the northwest corner of a GEOS-Chem grid box. Therefore, the results of the grid box including Halifax and the ones to the north and the west are presented below.

3 FTS measurements of CO and C_2H_6 during July 2011

Figure 2a shows the Halifax time series (for July 2011) of the total column CO observed by PARIS-IR, DAO-DA8 and IASI, and the total column C_2H_6 from DAO-DA8. The estimated total uncertainties are also shown as black bars (as listed in Table 1 and in Sect. 2.4 for the ground-based FTSs and IASI, respectively). The measurements from the ground and the satellite show a consistent enhancement of CO and C_2H_6 over Halifax on 19, 20 and 21 July 2011 (shown in Fig. 2b). The columns of CO and C_2H_6, seen on 20 and 21 July, are significantly enhanced compared to the background values of approximately 1.8×10^{18} molec cm^{-2} and 1.1×10^{16} molec cm^{-2}, respectively. These background columns are based on average values for July 2011 over Halifax from the ground-based FTSs. The majority of the ground-based observations from the two FTSs agree well within the estimated uncertainties. For coincident measurements ($\Delta t \leq 5$ min) during July 2011, the mean relative difference between DAO-DA8 and PARIS-IR total column CO measurements is $-4.9\pm0.7\%$. This difference was calculated as ([PARIS − DAO-DA8]/[0.5 · (PARIS + DAO-DA8)]) using around 150 pairs of measurements. The mean relative difference between PARIS-IR and IASI total column CO is $7.5\pm1.6\%$ for July 2011. This was calculated as ([PARIS − IASI]/[0.5 · (PARIS + IASI)]) using about 40 pairs of coincident measurements ($\Delta t \leq 15$ min). During the period of the enhanced CO columns, between 19 and 23 July, the mean difference between PARIS-IR and DAO-DA8 is $-9.9\pm0.7\%$ (using around 25 pairs). For PARIS-IR and IASI measurements taken over the same time period, the mean relative difference in total column CO is $19.2\pm1.6\%$ (calculated as described above), using seven pairs of measurements of coincident measurements ($\Delta t \leq 15$ min). The uncertainty given is the standard error for each calculation.

A more adequate comparison has been made by "smoothing" the retrieved profiles in order to account for the different sensitivities of the spectrometers, as described in Sect. 2.5. The CO total columns from PARIS-IR, DAO-DA8 and IASI, the latter two having been smoothed with PARIS-IR's averaging kernel and a priori profile, are shown in Fig. 2c. This shows an improved agreement between these two ground-based FTSs, as well as IASI, compared to the unsmoothed columns, which is shown in Fig. 2b. The mean relative difference in the total column CO between DAO-DA8 and PARIS-IR (as calculated above) reduces to $-3.5\pm0.7\%$ for July and to $-4.0\pm1.2\%$ during the enhancement period (mean ± standard error), respectively, after the smoothing procedure, using the same pairs of measurements as above. The differences between the total columns measured by two ground-based FTSs are very small and within the combined estimated uncertainties after the smoothing procedure (see Table 1). The mean relative difference between the total column CO results from PARIS-IR and IASI (calculated as above for 19–23 July) decreases to $6.6\pm1.8\%$ for July and $11.7\pm5.1\%$ during the enhanced period (mean ± standard error) after the smoothing procedure, using the same pairs of measurements as above. After taking the different sensitivities of the instruments into account using the averaging kernels, the difference between the total column CO of PARIS-IR and IASI is smaller and within the estimated uncertainty of IASI (3–9 %; see Sect. 2.4). Kerzenmacher et al. (2012) found slightly smaller mean differences (typically between ±2 %) between ground-based FTS measurements and IASI for three different mid-latitude NDACC FTS sites. The relatively large mean difference and the high standard deviation (±13 %) for the comparison between PARIS-IR and IASI is possibly due to the small number of pairs which have been used for this calculation; Kerzenmacher et al. (2012) used over 1000 pairs of total and partial columns from each measurement site to compare with IASI.

The time series of total column CO and C_2H_6 from the TAO-DA8 and IASI total column CO at Toronto are shown in Fig. 3a. Observations made over Toronto show enhancements of CO on 19 and 20 July, and enhancements of C_2H_6 on 21 and 22 July 2011 (shown in Fig. 3b). These are the same days when the columns observed in Halifax were enhanced. On 21 July, the total column C_2H_6 is almost twice as much as the typical background amount in Toronto ($\sim 1.5\times10^{16}$ molec cm^{-2}, based on July 2011 average). The CO total columns from the TAO-DA8 do not show a strong enhancement, which is due to the limited number of observations in this period; only three CO measurements are available between 20 and 22 July 2011. Slightly enhanced CO columns were detected by IASI near Toronto on 19 July and early in the morning on 20 July 2011. The CO enhancement on 19 and 20 July near Toronto is not as large as that detected near Halifax. Very little or no enhancement was seen on the other days in July 2011. The total column CO from IASI agrees with the ground-based observations from TAO-DA8 within the estimated uncertainties (see Table 1 and Sect. 2.4) on 20 and 21 July; however, on 19 July, IASI detects enhanced CO columns, which are not picked up by the ground-based measurements. However, the lowest detected IASI CO columns at this time are almost within the combined estimated uncertainties of the two instruments.

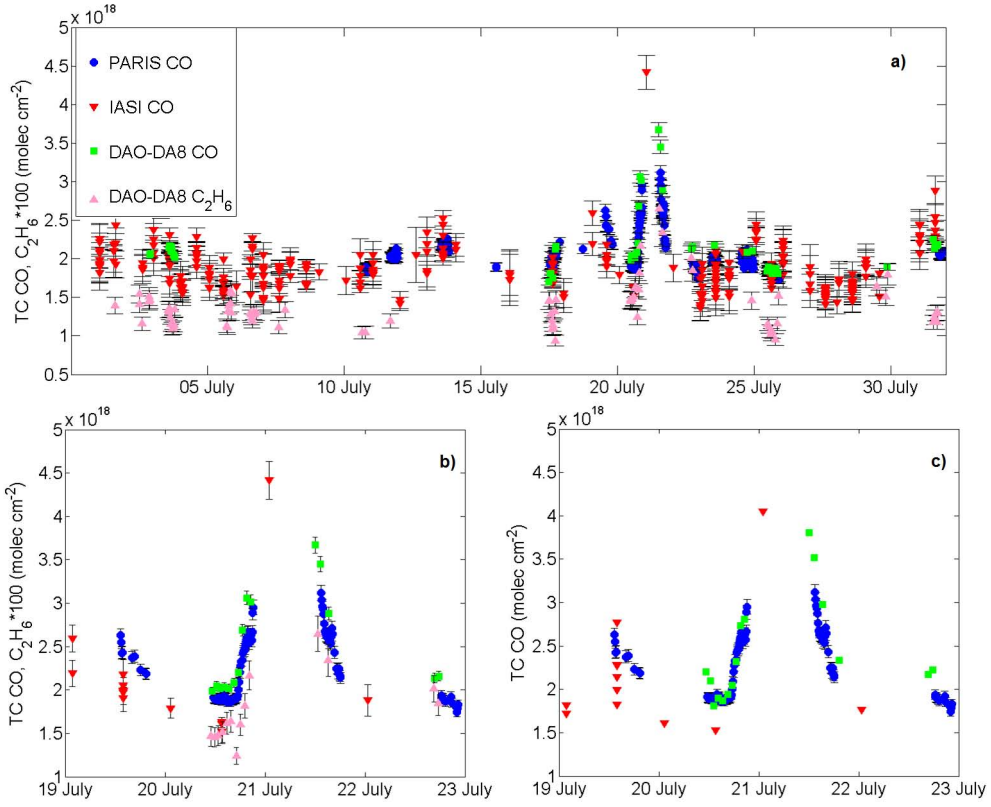

Fig. 2. The total column measurements (TC) in Halifax are shown for CO and C_2H_6 for **(a)** July 2011, **(b)** between 19 and 23 July 2011, and **(c)** CO total columns of DAO-DA8 and IASI smoothed with the PARIS-IR averaging kernel. PARIS-IR (blue dots), IASI (red inverted triangles), DAO-DA8 (green squares) total columns for CO, and DAO-DA8 total columns for C_2H_6 (pink triangles) are shown. The labels on the x axes indicate the start of each day at 00:00 UTC. Note that the C_2H_6 columns are scaled by a factor of 100 in panels **(a)** and **(b)**. The black bars indicate the estimated uncertainties for each gas and instrument, as described in Table 1 and Sect. 2.4.

4 Results and discussion

Enhancements of CO and C_2H_6 as seen in the observations from the ground-based FTSs and IASI over Halifax and Toronto are usually indicators of smoke plumes. To identify where this smoke originated, satellite-based measurements of fire hotspots during this time period, as well as trajectory calculations from CMC and FLEXPART, have been used. This section also includes a regression analysis for CO and C_2H_6 with respect to the fine-mode AOD, an estimate of the C_2H_6 emission ratio and factor, and a comparison with GEOS-Chem.

4.1 Origin of the enhanced trace gas columns

The FLAMBE inventory (Reid et al., 2009) was used to estimate the location and the total carbon emissions from boreal fires during the BORTAS-B campaign in 2011. This inventory provides hourly estimates of carbon and aerosol emissions based on observations from the Geostationary Operational Environmental Satellite (GOES) platforms and the two Moderate Resolution Imaging Spectrometers (MODIS) on the NASA EOS Terra and Aqua satellites. Figure 4 shows the daily carbon emissions obtained from the combined GOES and MODIS dataset between 7 July and 31 July 2011 from boreal fire regions ($\geq 50°$ N). The majority of boreal fire emissions from 17 to 20 July originated from fires in eastern Siberia and Canada, where emissions from northwestern Ontario essentially dominate the total Canadian emissions. The carbon emission from boreal fires in northwestern Ontario peaks on 17 July 2011 at a value of approximately 5 Tg C. At the same time, carbon emissions from eastern Siberia reach values of over 10 Tg C. Assuming a wind speed of 10–15 m s^{-1}, the approximate time it takes for smoke plumes originating from eastern Siberia and northwestern Ontario to reach Halifax is of the order of one week and 1–2 days, respectively.

Figure 5 shows an ensemble of back trajectories from Environment Canada's CMC long-range transport model (D'Amours and Pagé, 2001; D'Amours, 1998). These model outputs are provided in 6 h intervals over a 72 h period, and illustrate the origin of the air parcel overpassing Halifax at 18:00 UTC on 19 to 22 July 2011 at altitudes between 1 and 10 km. Between 19 and 21 July 2011, the air parcels at altitudes between 3 and 5 km originate from the area of forest

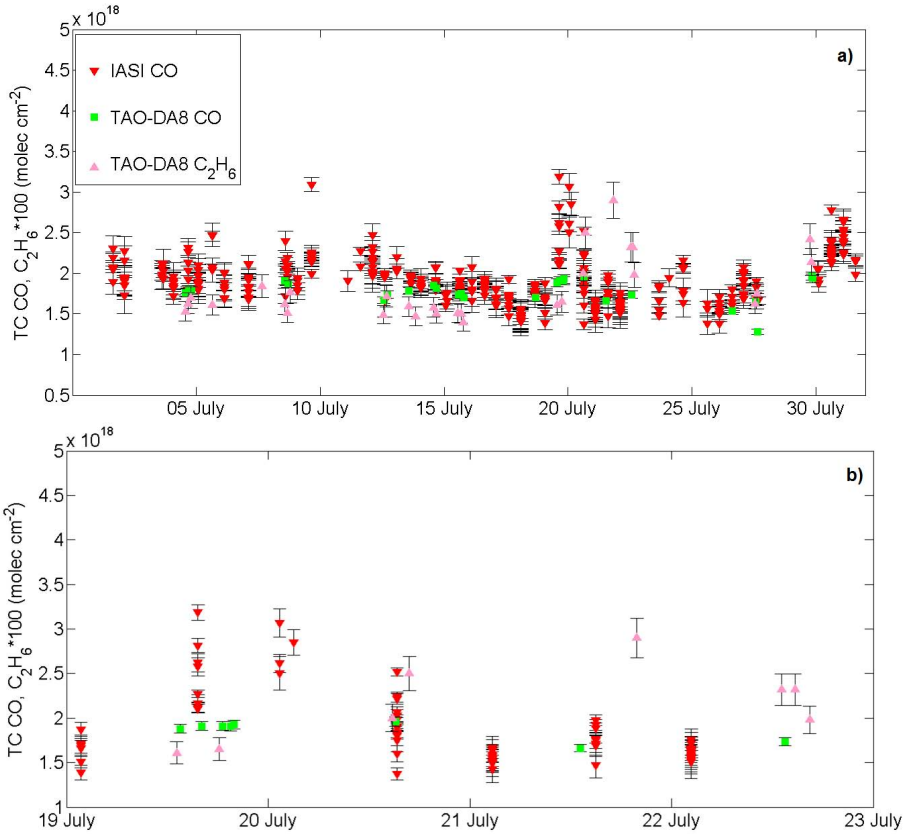

Fig. 3. The total column (TC) measurements in Toronto are shown for CO and C_2H_6 for **(a)** July 2011 and **(b)** between 19 and 22 July 2011. CO from TAO-DA8 (green squares), CO from IASI (red inverted triangles), and C_2H_6 from TAO-DA8 (pink triangles) are shown. The labels on the *x* axes indicate the start of the day at 00:00 UTC. Note that the C_2H_6 columns are scaled by a factor of 100. The black bars indicate the estimated uncertainties for each gas and instrument, as described in Table 1 and Sect. 2.4.

fires. According to these trajectory calculations, it took approximately 36 h ± 6 h, depending on the altitude of the air parcel, for the air parcel from the fire region in northwestern Ontario (50°–55° N, 95°–80° W) to arrive over Halifax. On 22 July 2011, the CMC back trajectories show that the tropospheric air parcels originated from an area south of the forest fires (Fig. 5d). This is consistent with our observations that no enhancement of CO or C_2H_6 was detected in Halifax in the evening of 22 July (see Fig. 2).

Further evidence of the origin of the CO and C_2H_6 enhancement between the 19 and 21 July 2011 can be seen in the FLEXPART forward trajectories, as well as IASI CO total columns. FLEXPART is a Lagrangian particle dispersion model, which was developed at the Norwegian Institute for Air Research (Stohl et al., 1998). FLEXPART was used to simulate forward trajectories for a constant particle release starting on 17 July 2011 at 12:00 UTC in northwestern Ontario (a continuous animation is available as supplementary material). Figure 6a and c show the results of this simulation at 15:00 UTC on 20 July 2011 and 21 July 2011, respectively. The forward trajectories from FLEXPART are consistent with the ground-based measurements, where small enhancements of CO and C_2H_6 occur on 19 July, followed by stronger enhancements on 20 (after 18:00 UTC) and 21 July 2011 in Halifax; and enhancements of C_2H_6 are seen in Toronto on 19 and 20 July 2011. The IASI CO total columns for the morning overpass (approximately 14:00 UTC) are shown in Fig. 6b and d for 20 July and 21 July 2011, respectively. The CO enhancements near Halifax seen from IASI show a similar pattern to the simulated trajectories from FLEXPART and support the assertion that these enhancements originated from the forest fires in northwestern Ontario.

4.2 Correlation between column amounts of trace gases and fine-mode AOD

As described in Sect. 1, trace gases, such as CO and C_2H_6 and the fine-mode AOD, emitted from biomass burning, are highly correlated for plumes younger than the lifetime of the aerosols, so approximately 5 days. Figure 7a shows the total column CO from PARIS-IR, the total column C_2H_6 from DAO-DA8 and measurements of fine-mode AOD, between 19 and 22 July 2011 at DGS. It can be seen that

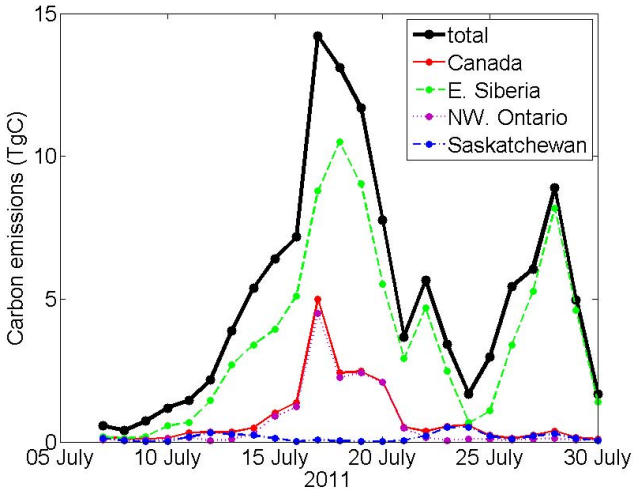

Fig. 4. Daily distribution of carbon emissions from the FLAMBE inventory based on fire information from MODIS and GOES. The traces show the daily total carbon emitted from all boreal fire regions (≥ 50° N, thick black line), for all of Canada (50°–75° N, 170°–50° W, thin red line), northwestern Ontario (50°–55° N, 95°–80° W, dotted purple line), Saskatchewan (55°–65° N, 120°–105° W, dot-dashed blue line), and eastern Siberia (50°–75° N, 110°–179° E, dashed green line).

the fine-mode AOD is enhanced during this time period, with a maximum of approximately 1 on 21 July. The typical background fine-mode AOD is approximately 0.05 at the DGS (based on July 2011 average background). Plots of the correlation between total column CO from PARIS-IR and total column C_2H_6 from DAO-DA8 with simultaneous, co-located measurements of the fine-mode AOD are shown in Fig. 7b and c, respectively. For these plots, the maximum temporal difference is less than 5 min between the measurements from the FTSs and the sun photometer. The points in Fig. 7b and c are colour coded to identify each of the days between 17 and 25 July 2011. These correlation plots show two different behaviours in the trace gas and fine-mode AOD enhancements. Most of the days show a similar relationship between the trace gases and AOD. However, on 20 July, the CO and C_2H_6 columns are high but the AOD is not significantly enhanced. The reason for this is likely a precipitation event (Franklin et al., 2013) in which most aerosols were removed, while the trace gas column stayed enhanced. After excluding data from this day, the simultaneous CO columns and the fine-mode AOD are highly correlated ($R^2 \approx 0.8$), with a slope of $(1.22 \pm 0.04) \times 10^{18}$ molec cm^{-2} per unit increase in fine-mode AOD and an intercept of $(1.76 \pm 0.01) \times 10^{18}$ molec cm^{-2}. More than 200 pairs, shown in Fig. 7b, were included in this calculation. Excluding the measurements from 20 July, the C_2H_6 columns measured by DAO-DA8 and simultaneous fine-mode AOD measurements are correlated ($R^2 \approx 0.7$) with a slope of $(1.6 \pm 0.2) \times 10^{16}$ molec cm^{-2} per unit increase in fine-mode AOD and an intercept of $(1.0 \pm 0.1) \times 10^{16}$ molec cm^{-2}, as shown in Fig. 7c. This lower correlation constant is possibly due to the limited number of enhanced C_2H_6 measurements from DAO-DA8, which makes it more difficult to determine the correlation of C_2H_6 against the fine-mode AOD. There are only 27 measurements of C_2H_6 available, which were taken between 17 and 25 July 2011. Of these, there are only two measurements which were taken when the smoke plume passed over Halifax on 21 July 2011.

In Toronto, only seven C_2H_6 measurements are available during this period. The enhancement seen in both the C_2H_6 total column and the fine-mode AOD is not as strong as in Halifax. The slope, obtained from a correlation plot of these results, suggests a similar trend between the C_2H_6 and fine-mode AOD as was seen in Halifax. However, there are not enough data available to analyse the correlation quantitatively.

4.3 Estimation of emission ratio and equivalent emission factor for C_2H_6

Trace gas concentrations from biomass burning plumes can vary significantly over a short period of time. However, the overall ratio between constituents within the plume is constant if no chemical reactions occur. Therefore, the concentrations of these trace gases are typically converted into relative emission ratios. These emission ratios are relative to a non-reactive co-emitted tracer, typically either CO or CO_2. Here, we use CO as a reference gas to estimate the emission ratio and emission factor of C_2H_6 from the boreal fire in northwestern Ontario.

The emission ratio is defined as the excess amount of a trace gas, in this case C_2H_6, over its background level divided by the excess amount of CO over its background level (Andreae and Merlet, 2001). Typically, emission ratios are measured at the fire source. The emission ratio measured further away from the source is called the enhancement ratio (Hobbs et al., 2003). However, since C_2H_6 is a long-lived species, the difference between the emission ratio and the enhancement ratio is negligible for a smoke plume that is approximately 1.5 days old (as estimated in Sect. 3). The emission ratio could also be obtained from the correlation slope between CO and C_2H_6. Here we calculate the emission ratio from the excess amounts of the trace gases, since there are not enough coincident measurements of CO and C_2H_6 available to get a reliable correlation coefficient.

For this estimation, the background levels for CO and C_2H_6 are obtained from the regression plots of the trace gas columns with respect to the fine-mode AOD (Fig. 7b and c) using a similar method to Paton-Walsh et al. (2005). Furthermore, we have used CO columns from PARIS-IR rather than from DAO-DA8 to obtain coincident measurements with a temporal difference less than 5 min. If this calculation was done using only results from DAO-DA8, the temporal difference between the CO and C_2H_6 measurements would need

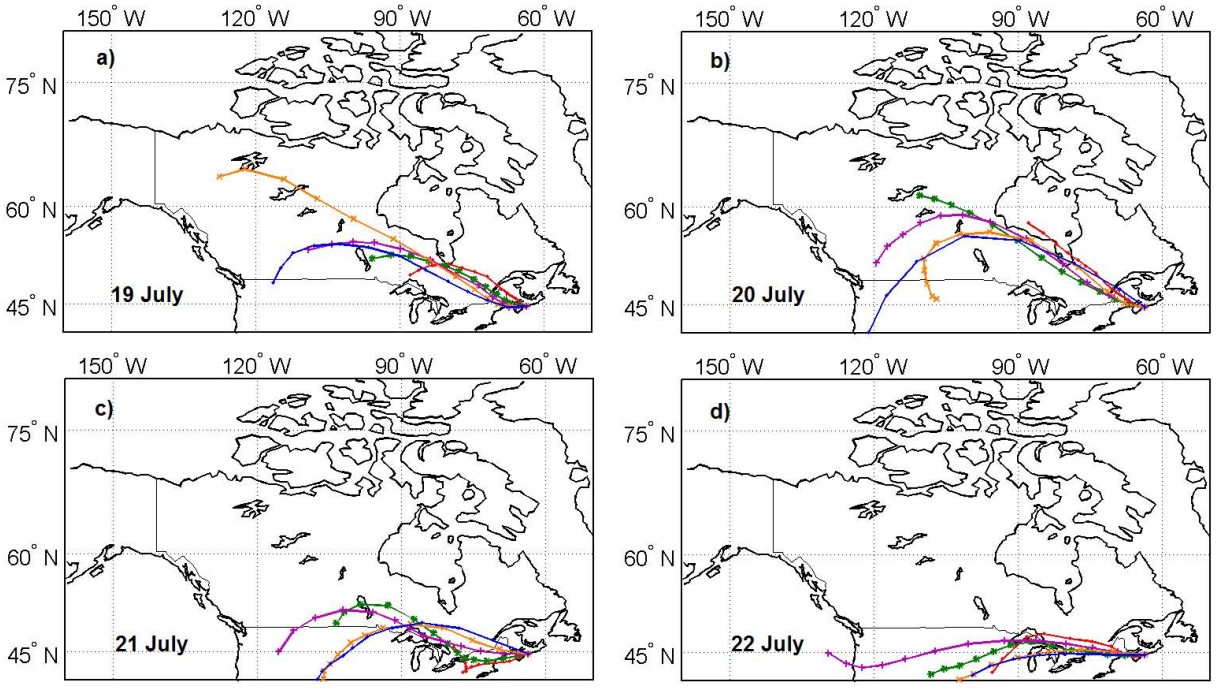

Fig. 5. Back trajectories from the CMC transport model. The back trajectories correspond to the origin of the air parcel overpassing Halifax at 18:00 UTC on **(a)** 19 July, **(b)** 20 July, **(c)** 21 July and **(d)** 22 July 2011 at altitudes of 10 km (orange crosses), 7 km (blue dots), 5 km (purple plus signs), 3 km (green stars) and 1 km (red dots). The markers indicate the location of the air parcel every 6 h over a 72 h period.

to increase to approximately 30 min. In this time, the trace gas columns can change significantly (see Fig. 2). Furthermore, we found that the CO columns from PARIS-IR and DAO-DA8 compare within the estimated uncertainties (see Sect. 3).

For the background level of the fine-mode AOD, we have chosen 0.05 (see Sect. 4.2). However, this value is not very critical for the calculation as it is very low. Our estimated background levels are 1.8×10^{18} molec cm^{-2} and 1.1×10^{16} molec cm^{-2} for CO and C_2H_6, respectively. These estimates agree well with the estimates of the background level obtained by averaging the background total columns for CO and C_2H_6 in July 2011 (see Sect. 3). For each pair of coincident PARIS-IR CO and DAO-DA8 C_2H_6 columns, we say that measurements were taken inside the boreal fire plume if the CO total column exceeds 2.2×10^{18} molec cm^{-2}. We divide the excess C_2H_6 amounts by the excess CO amounts to determine the emission ratio. The calculated emission ratio of C_2H_6 is $(10\pm6)\times10^{-3}$, which has been calculated from four measurement pairs (which were taken on 20 and 21 July 2011). This emission ratio $ER_{C_2H_6/CO}$ can be converted into an emission factor, $EF_{C_2H_6}$, using

$$EF_{C_2H_6} = ER_{C_2H_6/CO} \cdot (MW_{C_2H_6}/MW_{CO}) \cdot EF_{CO}, \quad (2)$$

where MW is the molecular weight of each species. The CO emission factor (in units of g CO per kg charcoal made) EF_{CO} is taken to be 122 ± 45 g kg^{-1} for extra-tropical forest fires (Akagi et al., 2011). Hence, the emission factor $EF_{C_2H_6}$ is determined to be 1.35 ± 0.51 g kg^{-1}. This value compares reasonably well (within the combined estimated uncertainties) to the result reported by Akagi et al. (2011) for boreal fires ($EF_{C_2H_6} = 1.8\pm1.2$ g kg^{-1}). This emission factor estimated by Akagi et al. (2011) has been derived from a combination of ground-based in situ ($EF_{C_2H_6} = 3.0\pm2.3$ g kg^{-1}) and airborne ($EF_{C_2H_6} = 0.6\pm0.3$ g kg^{-1}) measurements.

Emission ratios have been derived from airborne measurements (Lewis et al., 2013), as well as from satellite-based observations (Tereszchuk et al., 2013), for the same fire plume from northwestern Ontario during BORTAS-B. Their results for the emission ratio of C_2H_6 with respect to CO ($ER_{C_2H_6/CO} = (5.1\pm0.4)\times10^{-3}$ (Lewis et al., 2013) and $ER_{C_2H_6/CO} = (6.8\pm1.1)\times10^{-3}$ (Tereszchuk et al., 2013)) agree within the uncertainties with our estimates from ground-based FTS measurements, and are consistent with the emissions of C_2H_6 from airborne measurements of boreal fire plumes (Akagi et al., 2011).

4.4 Comparison between ground-based observations and GEOS-Chem

GEOS-Chem is a valuable tool for evaluating the chemistry within the atmosphere, and is often used to analyse the impact of biomass burning on tropospheric chemistry (e.g. Parrington et al., 2012). Here, we analyse the simulated CO and C_2H_6 columns from biomass burning using this chemical transport model (with the FLAMBE inventory), and evaluate

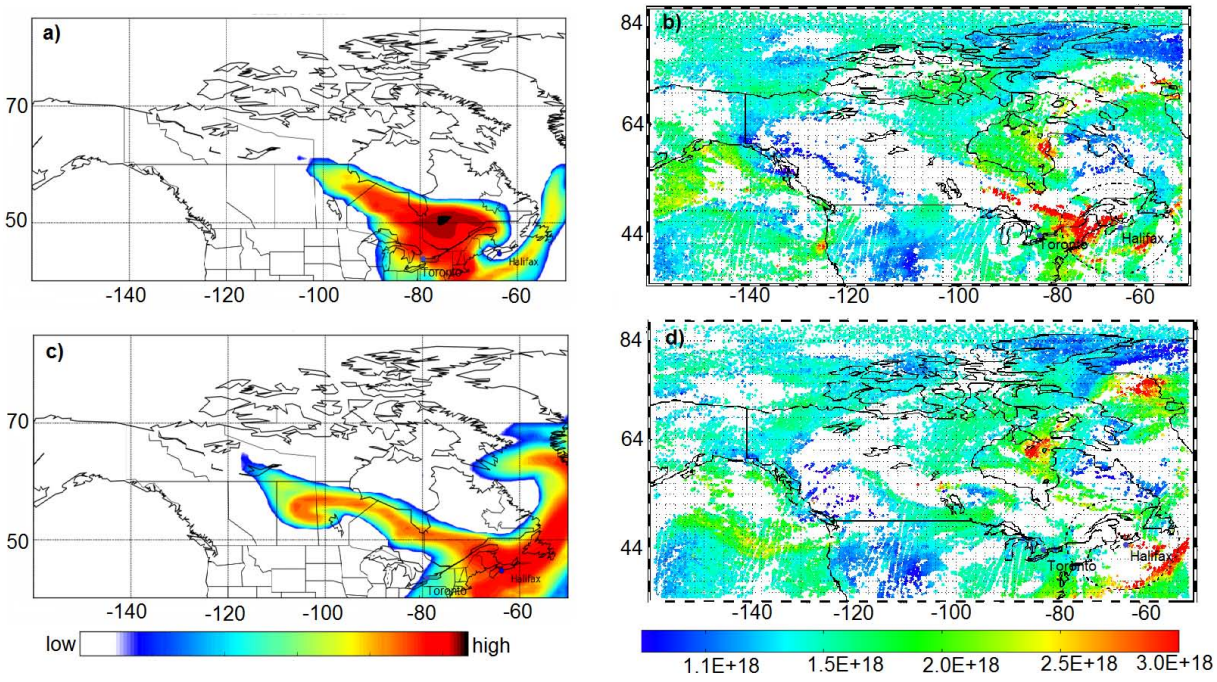

Fig. 6. FLEXPART forward trajectories at 15:00 UTC on **(a)** 20 July and **(c)** 21 July 2011, for a constant particle release starting on 17 July 2011 at 12:00 UTC. The colour contours are on a relative scale from high (red) to low (blue) low concentrations. IASI CO total columns in molec cm^{-2} on **(b)** 20 July and **(d)** 21 July 2011 for the morning overpass (approximately 14:00 UTC).

how these compare with ground-based measurements in Halifax. We validate the model simulations by using our ground-based measurements during the fire plume event. The model simulation for three nearby grid boxes – over Halifax, west of Halifax and north of Halifax – and the results from PARIS-IR in the period between 19 and 22 July 2011 are shown in Fig. 8a. The GEOS-Chem profiles have been smoothed with the PARIS-IR averaging kernel using the method described in Sect. 2.5 and integrated to obtain total columns. The agreement between PARIS-IR and the smoothed GEOS-Chem total column CO seems to be best for the GEOS-Chem grid box to the north of Halifax. An increase in CO after 18:00 UTC on 20 July 2011 and a decrease on 21 July 2011 can be seen in both the measurements and the model output. However, the CO enhancement from the model simulation seems to reach Halifax with a delay of approximately 6 h compared to the measurements. The magnitude of the modelled CO enhancement (peak column of approximately 3.2×10^{18} molec cm^{-2}) compares well with the measurements within the stated measurement uncertainty (peak column of $(3.12 \pm 0.09) \times 10^{18}$ molec cm^{-2}) . A possible reason for the discrepancy between the measured and simulated CO columns is the relatively large grid box of GEOS-Chem, since the intensity of a relatively young fire plume (of a few days) can vary significantly over a relatively small area. GEOS-Chem is currently being used to perform simulations at a higher horizontal resolution of 0.5° latitude × 0.67° longitude, covering the geographical extent of the BORTAS aircraft and ground-based measurements. This type of discrepancy might be reduced with the high-resolution model simulation, which may lead to a better comparison between the model and the ground-based observations.

The measured C_2H_6 total columns from the DAO-DA8 and simulated total columns of C_2H_6 from GEOS-Chem are shown in Fig. 8b. As was done for the CO comparisons, the simulated profiles from GEOS-Chem were smoothed with the DAO-DA8 averaging kernel for C_2H_6 before calculating the total columns (see Sect. 2.5 for details). The C_2H_6 columns do not differ significantly for the different grid boxes, and therefore only the simulation over Halifax is shown. The emission ratio of C_2H_6 used in the GEOS-Chem simulations ($ER_{C_2H_6/CO} = 5.6 \times 10^{-3}$, Andreae and Merlet, 2001) is similar to the emission ratio obtained in this study for this boreal fire plume ($ER_{C_2H_6/CO} = (10 \pm 6) \times 10^{-3}$). The comparison shows that during the enhanced periods on 20 and 21 July 2011, the simulated C_2H_6 columns agree well with the observations within the estimated measurement uncertainty of approximately 8 %. However, the simulated columns are also enhanced earlier on 19 and 20 July 2011.

5 Summary and conclusions

We have presented total column measurements of CO and C_2H_6, as well as fine-mode AOD, obtained using ground-based FTSs, a space-based emission spectrometer (IASI) and

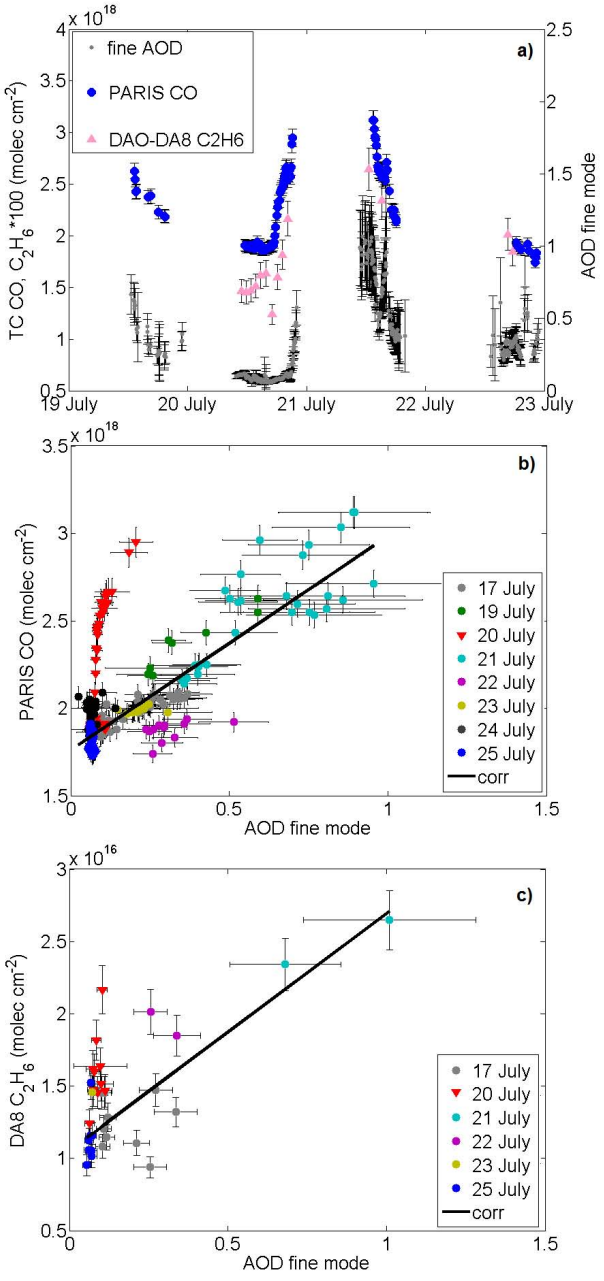

Fig. 7. Panel **(a)** shows total columns for CO from PARIS-IR (blue circles) and C_2H_6 from DAO-DA8 (pink triangles) over Halifax between 19 and 22 July 2011 (axis on left). The grey dots correspond to the fine-mode AOD (axis on the right) over Halifax. The labels on the *x* axis indicate the start of each day at 00:00 UTC. Note that the C_2H_6 columns are scaled by a factor of 100. Panel **(b)** shows the correlation between PARIS-IR CO total columns and the fine-mode AOD. Panel **(c)** shows the correlation between DAO-DA8 C_2H_6 total columns and the fine-mode AOD. In panels **(b)** and **(c)**, the thick black line corresponds to the linear regression fit (see Sect. 4.2). Note that for this calculation, measurements on 20 July 2011 (red inverted triangles) are excluded. Black bars indicate the estimated uncertainties, as described in Table 1 and Sect. 2.6.

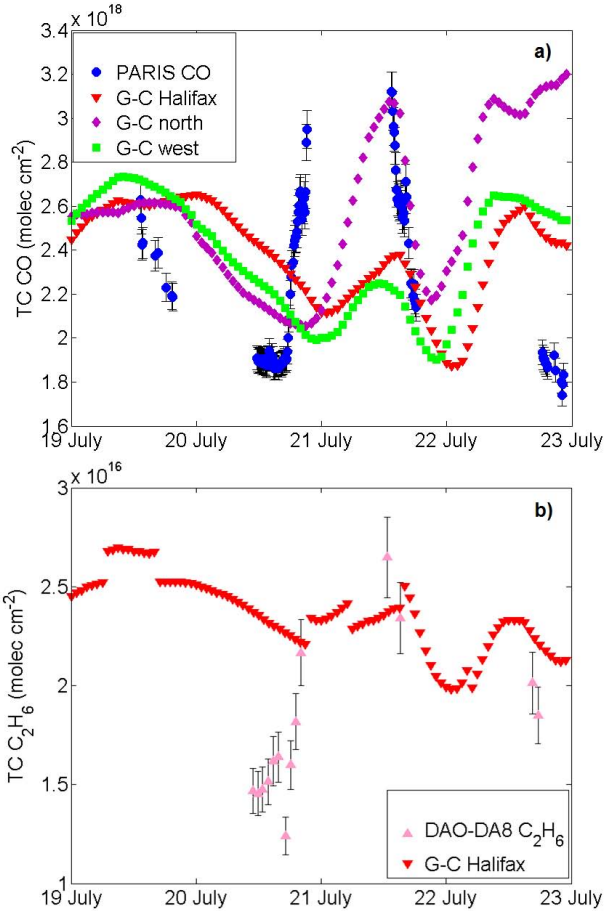

Fig. 8. Panel **(a)** shows the total column CO from PARIS-IR (blue circles) and GEOS-Chem for the grid box above Halifax (red inverted triangles), north of Halifax (purple diamonds) and west of Halifax (green squares) between 19 and 22 July 2011 UTC. Panel **(b)** shows the total column C_2H_6 from DAO-DA8 (pink triangles), and the C_2H_6 total columns of the GEOS-Chem simulation (red inverted triangles) above Halifax. Note that the difference between C_2H_6 for the three GEOS-Chem grid boxes is not significant; therefore, only the simulation over Halifax is shown. The profiles from the GEOS-Chem simulations have been smoothed with PARIS (for CO) and DAO-DA8 (for C_2H_6) averaging kernels before calculating the total columns; see Sect. 2.5 for details on the smoothing procedure. The black bars indicate the estimated uncertainty for each gas and ground-based instrument, as listed in Table 1.

sun photometers. Enhancements of the total column CO, C_2H_6 and the fine-mode AOD could be seen over Halifax on 19, 20 and 21 July 2011. On the same days, enhancements of these trace gases and the fine-mode AOD could be seen over Toronto. The two ground-based FTSs in Halifax agree well within the estimated uncertainties for the CO total columns, for which the mean difference is much improved once the different vertical sensitivities of the measurements have been considered. The difference between ground-based FTS (PARIS-IR) measurements and the

space-based IASI measurements is improved after applying the smoothing procedure using PARIS-IR's averaging kernel. However, the mean difference and standard deviation are quite large, which is possibly due to the limited coincident measurements (seven coincident measurements) between 19 and 22 July 2011.

During this time period, MODIS and GOES detected fire activities in eastern Siberia and northwestern Ontario. Using CMC back trajectories and FLEXPART forward trajectories, we identified the source of the trace gas enhancements over Halifax and Toronto to be boreal fires in northwestern Ontario. Furthermore, the high correlation between the trace gases and the fine-mode AOD is consistent with our arguments concerning the effective lifetimes of smoke aerosols and CO and C_2H_6 trace gases being less than 5 days. The transportation time between the source – northwestern Ontario – and Halifax was approximately 36 h according to the simulated trajectories from CMC and FLEXPART.

Our estimated emission ratio and emission factor for C_2H_6 ($ER_{C_2H_6/CO} = (10 \pm 6) \times 10^{-3}$, $EF_{C_2H_6} = 1.35 \pm 0.51\,g\,kg^{-1}$) for the boreal fire in northwestern Ontario are consistent with other studies. Our values agree within the estimated uncertainties with the results from Akagi et al. (2011) ($EF_{C_2H_6} = 1.8 \pm 1.2\,g\,kg^{-1}$) for the C_2H_6 emission factor from boreal fires, but they are significantly higher compared to other geographical regions, e.g. from Australian wildfires ($EF_{C_2H_6} = 0.26 \pm 0.11\,g\,kg^{-1}$, Paton-Walsh et al., 2005). Estimated emission ratios from the same smoke plume based on airborne as well as satellite measurements ($ER_{C_2H_6/CO} = (5.1 \pm 0.4) \times 10^{-3}$, Lewis et al., 2013, and $ER_{C_2H_6/CO} = (6.8 \pm 1.1) \times 10^{-3}$, Tereszchuk et al., 2013) are lower than our results, but agree within the estimated uncertainties.

These results are consistent with the comparison between GEOS-Chem simulations and the FTS observations for the C_2H_6 total columns. Employing an emission ratio of C_2H_6 with respect to CO of 5.6×10^{-3} for extra-tropical fires (Andreae and Merlet, 2001) in the GEOS-Chem simulation, the simulated peak C_2H_6 total columns are similar to the coincident observed peak values on 20 and 21 July 2011. However, the lower C_2H_6 total columns on 20 July 2011 are not as well simulated. The transport and chemistry of CO emitted by the boreal fire in northwestern Ontario could be simulated reasonably well with GEOS-Chem, as the comparisons between the observed and simulated CO total columns show. We found that the GEOS-Chem grid box north of Halifax represents the observations from the DGS the best. The ground-based FTS measurements and GEOS-Chem agree well in the magnitude of the CO total columns. However, there are differences in the timing of the enhancement, where the model simulation shows CO enhancements approximately 6 h after the measured total columns CO enhancements on 20 July 2011.

Supplementary material related to this article is available online at http://www.atmos-chem-phys.net/13/10227/2013/acp-13-10227-2013-supplement..zip.

Acknowledgements. Funding for this work has been provided by a grant from the Natural Sciences and Engineering Research Council of Canada (NSERC). Funding for the DGS measurements has been provided by NSERC, the Canadian Space Agency (CSA) and Environment Canada (EC). The BORTAS project is funded by the Natural Environment Research Council under grant NE/F017391/1. The TAO measurements were made with support from NSERC, CSA and EC. IASI has been developed and built under the responsibility of the Centre National des Etudes Spatiales (CNES, France). P.-F. Coheur is a Research Associate with Fonds de la Recherche Scientifique (FRS-FNRS); his work is also supported by the Belgian Science Policy Office through ESA-Prodex C4000103226 arrangement. We would like to further acknowledge the LATMOS research group for providing the level 2 IASI CO data. We are also very grateful to AEROCAN (Environment Canada and the Université de Sherbrooke) and AERONET (NASA/GSFC) for their support and commitment to their respective networks, as well as to Mike Boschat for operating the CIMEL in Halifax for many years. We also acknowledge the work of David Waugh and Jacinthe Racine, who carried out the analysis of the CMC back trajectories and provided us with these data.

Edited by: S. Matthiesen

References

Akagi, S. K., Yokelson, R. J., Wiedinmyer, C., Alvarado, M. J., Reid, J. S., Karl, T., Crounse, J. D., and Wennberg, P. O.: Emission factors for open and domestic biomass burning for use in atmospheric models, Atmos. Chem. Phys., 11, 4039–4072, doi:10.5194/acp-11-4039-2011, 2011.

Andreae, M. O. and Merlet, P.: Emission of trace gases and aerosols from biomass burning, Global Biogeochem. Cy., 15, 955–966, 2001.

Batchelor, R. L., Strong, K., Lindenmaier, R. L., Mittermaier, R., Fast, H., Drummond, J. R., and Fogal, P. F.: A new Bruker 125HR FTIR spectrometer for the Polar Environment Atmospheric Research Laboratory at Eureka, Canada – measurements and comparison with the existing Bomem DA8 spectrometer, J. Atmos. Ocean. Technol., 26, 1328–1340, 2009.

Bey, I., Jacob, D. J., Yantosca, R. M., Logan, J. A., Field, B. D., Fiore, A. M., Li, Q. B., Liu, H. Y., Mickley, L. J., and Schultz, M. G.: Global modeling of tropospheric chemistry with assimilated meteorology: model description and evaluation, J. Geophys. Res.-Atmos., 106, 23073–23095, doi:10.1029/2001JD000807, 2001.

Clerbaux, C., Boynard, A., Clarisse, L., George, M., Hadji-Lazaro, J., Herbin, H., Hurtmans, D., Pommier, M., Razavi, A., Turquety, S., Wespes, C., and Coheur, P.-F.: Monitoring of atmospheric composition using the thermal infrared IASI/MetOp

sounder, Atmos. Chem. Phys., 9, 6041–6054, doi:10.5194/acp-9-6041-2009, 2009.

Crutzen, P. J. and Andreae, M. O.: Biomass burning in the tropics: Impact on atmospheric chemistry and biochemical cycles, Science, 250, 1669–1678, 1990.

D'Amours, R.: Modeling the ETEX plume dispersion with the Canadian emergency response model, Atmos. Environ., 32, 4335–4341, 1998.

D'Amours, R. and Pagé, P.: Atmospheric transport models for environmental emergencies, Canadian Meteorological Centre, available at: http://collaboration.cmc.ec.gc.ca/cmc/cmoi/product_guide/docs/lib/model-eco_urgences_e.pdf, last access: 18 April 2013, 2001.

Derwent, R. G., Stevenson, D. S., Collins, W. J., and Johnson, C. E.: Intercontinental transport and the origins of the ozone observed at surface sites in Europe, Atmos. Environ., 38, 1891–1901, 2004.

Edwards, D. P., Emmons, L. K., Gille, J. C., Chu, A., Attie, J.-L., Giglio, L., Wood, S. W., Haywood, J., Deeter, M. N., Massie, S. T., Ziskin, D. C., and Drummond, J. R.: Satellite-observed pollution from Southern Hemisphere biomass burning, J. Geophys. Res., 111, D14312, doi:10.1029/2005JD006655, 2006.

Eyring, V., Waugh, D. W., Bodeker, G. E., Cordero, E., Akiyoshi, H., Austin, J., Beagley, S. R., Boville, B. A., Braesicke, P., Brühl, C., Butchart, N., Chipperfield, M. P., Dameris, M., Deckert, R., Deushi, M., Frith, S. M., Garcia, R. R., Gettelman, A., Giorgetta, M. A., Kinnison, D. E., Mancini, E., Manzini, E., Marsh, D. R., Matthes, S., Nagashima, T., Newman, P. A., Nielsen, J. E., Pawson, S., Pitari, G., Plummer, D. A., Rozanov, E., Schraner, M., Scinocca, J. F., Semeniuk, K., Shepherd, T. G., Shibata, K., Steil, B., Stolarski, R. S., Tian, W., and Yoshiki, M.: Multimodel projections of stratospheric ozone in the 21st century, J. Geophys. Res., 112, D16303, doi:10.1029/2006JD008332, 2007.

Franklin, J. E., Griffin, D., Pierce, J. R., Drummond, J. R., Waugh, D. L., Palmer, P. I., Chisholm, L., Duck, T. J., Hopper, J. T., Gibson, M., Curry, K. R., Sakamoto, K. M., Lesins, G. L., Walker, K. A., Dan, L., Kliever, J., and O'Neill, N.: A case study of aerosol depletion in a biomass burning plume over Eastern Canada during the 2011 BORTAS field experiment, Atmos. Chem. Phys., to be submitted, 2013.

Fu, D., Walker, K. A., Sung, K., Boone, C. D., Soucy, M.-A., and Bernath, P. F.: The portable atmospheric research interferometric spectrometer for the infrared, PARIS-IR, J. Quant. Spectrosc. Ra., 103, 362–370, 2007.

George, M., Clerbaux, C., Hurtmans, D., Turquety, S., Coheur, P.-F., Pommier, M., Hadji-Lazaro, J., Edwards, D. P., Worden, H., Luo, M., Rinsland, C., and McMillan, W.: Carbon monoxide distributions from the IASI/METOP mission: evaluation with other space-borne remote sensors, Atmos. Chem. Phys., 9, 8317–8330, doi:10.5194/acp-9-8317-2009, 2009.

Hobbs, P. V., Sinha, P., Yokelson, R. J., Christian, T. J., Blake, D. R., Gao, S., Kirchstetter, T. W., Novakov, T., and Pilewskie, P.: Evolution of gases and particles from a savanna fire in South Africa, J. Geophys. Res., 108, D13, 8485, doi:10.1029/2002JD002352, 2003.

Holben, B. N., Eck, T. F., Slutsker, I., Tanré, D., Buis, J. P., Setzer, A., Vermonte, E., Reagan, J. A., Kaufman, Y. J., Nakajima, T., Lavenu, F., Jankowiak, I., and Smirnov, A.: AERONET – a ferderated instrument network and data archive for aerosol characterization, Remote Sens. Environ., 66, 1–16, 1998.

Hurtmans, D., Coheur, P.-F., Wespes, C., Clarisse, L., Scharf, O., Clerbaux, C., Hadji-Lazaro, J., George, M., and Turquety, S.: FORLI radiative transfer and retrieval code for IASI, J. Quant. Spectrosc. Ra., 113, 1391–1408, 2012.

Kerzenmacher, T., Dils, B., Kumps, N., Blumenstock, T., Clerbaux, C., Coheur, P.-F., Demoulin, P., García, O., George, M., Griffith, D. W. T., Hase, F., Hadji-Lazaro, J., Hurtmans, D., Jones, N., Mahieu, E., Notholt, J., Paton-Walsh, C., Raffalski, U., Ridder, T., Schneider, M., Servais, C., and De Mazière, M.: Validation of IASI FORLI carbon monoxide retrievals using FTIR data from NDACC, Atmos. Meas. Tech., 5, 2751–2761, doi:10.5194/amt-5-2751-2012, 2012.

Krol, M., Peters, W., Hooghiemstra, P., George, M., Clerbaux, C., Hurtmans, D., McInerney, D., Sedano, F., Bergamaschi, P., El Hajj, M., Kaiser, J. W., Fisher, D., Yershov, V., and Muller, J.-P.: How much CO was emitted by the 2010 fires around Moscow?, Atmos. Chem. Phys., 13, 4737–4747, doi:10.5194/acp-13-4737-2013, 2013.

Lewis, A. C., Evans, M. J., Hopkins, J. R., Punjabi, S., Read, K. A., Purvis, R. M., Andrews, S. J., Moller, S. J., Carpenter, L. J., Lee, J. D., Rickard, A. R., Palmer, P. I., and Parrington, M.: The influence of biomass burning on the global distribution of selected non-methane organic compounds, Atmos. Chem. Phys., 13, 851–867, doi:10.5194/acp-13-851-2013, 2013.

Li, Q., Jacob, D. J., Bey, I., Palmer, P. I, Duncan, B. N., Field, B. D., Martin, R. V., Fiore, A. M., Yantosca, R. M., Parrish, D. D., Simmonds P. G., and Oltmans, S. J. : Transatlantic transport of pollution and its effect on the surface ozone in Europe and North America, J. Geophys. Res., 107, D13, doi:10.1029/2001JD001422, 2002.

O'Neill, N. T., Eck, T. F., Smirnov, A., Holben, B. N., and Thulasiraman, S.: Spectral discrimination of coarse and fine mode optical depth, J. Geophys. Res., 108, D17, doi:10.1029/2002JD002975, 2003.

Palmer, P. I., Parrington, M., Lee, J. D., Lewis, A. C., Rickard, A. R., Bernath, P. F., Duck, T. J., Waugh, D. L., Tarasick, D. W., Andrews, S., Aruffo, E., Bailey, L. J., Barrett, E., Bauguitte, S. J.-B., Curry, K. R., Di Carlo, P., Chisholm, L., Dan, L., Forster, G., Franklin, J. E., Gibson, M. D., Griffin, D., Helmig, D., Hopkins, J. R., Hopper, J. T., Jenkin, M. E., Kindred, D., Kliever, J., Le Breton, M., Matthiesen, S., Maurice, M., Moller, S., Moore, D. P., Oram, D. E., O'Shea, S. J., Owen, R. C., Pagniello, C. M. L. S., Pawson, S., Percival, C. J., Pierce, J. R., Punjabi, S., Purvis, R. M., Remedios, J. J., Rotermund, K. M., Sakamoto, K. M., da Silva, A. M., Strawbridge, K. B., Strong, K., Taylor, J., Trigwell, R., Tereszchuk, K. A., Walker, K. A., Weaver, D., Whaley, C., and Young, J. C.: Quantifying the impact of BOReal forest fires on Tropospheric oxidants over the Atlantic using Aircraft and Satellites (BORTAS) experiment: design, execution and science overview, Atmos. Chem. Phys., 13, 6239–6261, doi:10.5194/acp-13-6239-2013, 2013.

Parrington, M., Palmer, P. I., Henze, D. K., Tarasick, D. W., Hyer, E. J., Owen, R. C., Helmig, D., Clerbaux, C., Bowman, K.W, Deeter, M. N., Barratt, E. M., Coheur, P.-F., Hurtsmans, D., Jiang, Z., George, M., and Worden, J. R.: The influence of boreal biomass burning emissions on the distribution of tropospheric ozone over North America and the North Atlantic during

2010, Atmos. Chem. Phys., 12, 2077–2098, doi:10.5194/acp-12-2077-2012, 2012.

Paton-Walsh, C., Jones, N. B., Wilson, S. R., Haverd, V., Meier, A., Griffith, D. W. T., and Rinsland, C. P.: Measurements of trace gas emissions from Australian forest fires and correlation with coincident measurements of aerosol optical depth, J. Geophys. Res., 110, D24305, doi:10.1029/2005JD006202, 2005.

Paton-Walsh, C., Wilson, S. R., Jones, N. B., and Griffith, D. W. T.: Measurements of methanol emissions from Australian wildfires by ground-based solar Fourier transform spectroscopy, Geophys. Res. Lett., 35, L08810, doi:10.1029/2007GL032951, 2008.

Pougatchev, N. S., Connor, B. J., and Rinsland, C. P.: Infrared measurements of the ozone vertical distribution above Kitt Peak, J. Geophys. Res., 100, 16689–16697, 1995.

Pougatchev, N. S., Connor, B. J., Jones, N. B., and Rinsland, C. P.: Validation of ozone profile retrievals from infrared ground-based solar spectra, Geophys. Res. Lett., 23, 1637–1640, 1996.

Reid, J. S., Hyer, E. J., Prins, E. M., Westphal, D. L., Zhang, J., Wang, J., Christopher, S. A., Curtis, C. A., Schmidt, C. C., Eleuterio, D. P., Richardson, K. A., and Hoffman, J. P.: Global monitoring and forecasting of biomass-burning smoke: Description of and lessons from the Fire Locating And Modeling of Burning Emissions (FLAMBE) program, IEEE J. Select. Topics Appl. Earth Obs. Remote Sens., 2, 144–162, 2009.

Rodgers, C. D.: Retrieval of atmospheric temperature and composition from remote measurements of thermal radiation, Rev. Geophys. Space Phys., 14, 609–624, 1976.

Rodgers, C. D.: Inverse Methods for Atmospheric Sounding – Theory and Practice, 2nd edn., World Scientific Publishing Co. Pte. Ltd., Danvers, USA, 2000.

Rodgers, C. D. and Connor, B. J.: Intercomparison of remote sounding instruments, J. Geophys. Res., 108, D3, 4116, doi:10.1029/2002JD002299, 2003.

Rothman, L. S., Gordon, I. E., Barbe, A., Benner, D. C., Bernath, P. F., Birk, M., Boudon, V., Brown, L. R., Campargue, A., Champion, J.-P., Chance, K., Coudert, L. H., Dana, V., Devi, V. M., Fally, S., Flaud, J.-M., Gamache, R. R., Goldman, A., Jacquemart, D., Kleiner, I., Lacome, N., Lafferty, W. J., Mandin, J.-Y., Massie, S. T., Mikhailenko, S. N., Miller, C. E., Moazzen-Ahmadi, N., Naumenko, O. V., Nikitin, A. V., Orphal, J., Perevalov, V. I., Perrin, A., Predoi-Cross, A., Rinsland, C. P., Rotger, M., Šimečková, M., Smith, M. A. H., Sung, K., Tashkun, S. A., Tennyson, J., Toth, R. A., Vandaele, A. C., and Vander Auwera, J.: The HITRAN 2008 molecular spectroscopic database, J. Quant. Spectrosc. Ra., 110, 533–572, 2009.

Rudolph, J. and Ehhalt, D. H.: Measurements of C_2-C_5 hydrocarbons over the North Atlantic, J. Geophys. Res., 86, 11959–11964, 1981.

Sinha, P., Hobbs, P. V., Yokelson, R. J., Bertschi, I. T., Blake, D. R., Simpson, I. J., Gao, S., Kirchstetter, T. W., and Novakov, T.: Emissions of trace gases and particles from savanna fires in southern Africa, J. Geophys. Res., 108, D13, 8487, doi:10.1029/2002JD002325, 2003.

Stohl A. and Trickl, T.: A textbook example of long-range transport: Simultaneous observation of ozone maxima of stratospheric and North American origin in the free troposphere over Europe, J. Geophys. Res., 104, D23, 30445–30462, 1999.

Stohl, A., Hittenberger, M., and Wotawa, G.: Validation of the lagrangian particle dispersion model FLEXPART against large scale tracer experiment data, Atmos. Environ. 32, 4245–4264, 1998.

Sung, K., Skelton, R., Walker, K. A., Boone, C. D., Fu, D., and Bernath, P. F.: N_2O and O_3 arctic column amounts from PARIS-IR observations: retrievals, characterization and error analysis, J. Quant. Spectrosc. Ra., 107, 385–406, 2007.

Tereszchuk, K. A., González Abad, G., Clerbaux, C., Hurtmans, D., Coheur, P.-F., and Bernath, P. F.: ACE-FTS measurements of trace species in the characterization of biomass burning plumes, Atmos. Chem. Phys., 11, 12169–12179, doi:10.5194/acp-11-12169-2011, 2011.

Tereszchuk, K. A., González Abad, G., Clerbaux, C., Hadji-Lazaro, J., Hurtmans, D., Coheur, P.-F., and Bernath, P. F.: ACE-FTS observations of pyrogenic trace species in boreal biomass burning plumes during BORTAS, Atmos. Chem. Phys., 13, 4529–4541, doi:10.5194/acp-13-4529-2013, 2013.

Turquety, S., Hurtmans, D., Hadji-Lazaro, J., Coheur, P.-F., Clerbaux, C., Josset, D., and Tsamalis, C.: Tracking the emission and transport of pollution from wildfires using the IASI CO retrievals: analysis of the summer 2007 Greek fires, Atmos. Chem. Phys., 9, 4897–4913, doi:10.5194/acp-9-4897-2009, 2009.

Volz, A., Ehhalt, D. H., and Derwent, R. G.: Seasonal and latitudinal variations of ^{14}CO and the tropospheric concentration of OH radicals, J. Geophys. Res., 86, 5163–5171, 1981.

Wiacek, A., Taylor, J. R., Strong, K., Saari, R., Kerzenmacher, T. E., Jones, N. B., and Griffith, D. W. T.: Ground-based solar absorption FTIR spectroscopy: characterization of retrievals and first results from a novel optical design instrument at a new NDACC complementary station, J. Atmos. Ocean. Technol., 24, 432–448, 2007.

Wunch, D., Taylor, J. R., Fu, D., Bernath, P., Drummond, J. R., Midwinter, C., Strong, K., and Walker, K. A.: Simultaneous ground-based observations of O_3, HCl, N_2O, and CH_4 over Toronto, Canada by three Fourier transform spectrometers with different resolutions, Atmos. Chem. Phys., 7, 1275–1292, doi:10.5194/acp-7-1275-2007, 2007.